Optimization, equilibrium and kinetic studies of Zn^{2+} and Ni^{2+} adsorption from aqueous solutions using composite adsorbent

Haider M. Zwain, Mohammadtaghi Vakili and Irvan Dahlan

ABSTRACT

A novel RHA/PFA/CFA composite adsorbent was synthesized from rice husk ash (RHA), palm oil fuel ash (PFA), and coal fly ash (CFA) by modified sol-gel method. Effect of different parameters such as adsorbent dosage, contact time, and pH were studied using batch experiment to optimize the maximum zinc (Zn^{2+}) and nickel (Ni^{2}) adsorption conditions. Results showed that the maximum adsorption condition occurred at adsorbent amount of 10 g/L, contact time of 60 min, and pH 7. At this condition, the removal efficiencies were 81% and 61% for Zn^{2+} and Ni^{2+}, in which the adsorption capacities (q_{max}) were 21.74 mg/g and 17.85 mg/g, respectively. Adsorption behavior of RHA/PFA/CFA composite adsorbent was studied through the various isotherm models at different adsorbent amounts. The results indicated that the Freundlich isotherm model gave an excellent agreement with the experimental conditions. Based on the results obtained from the kinetic studies, pseudo-second-order was suitable for the adsorption of Ni^{2+} and Zn^{2+}, compared to the pseudo-first-order model. The results presented in this study showed that RHA/PFA/CFA composite adsorbent successfully adsorbed Zn^{2+} and Ni^{2}.

Key words | adsorption isotherm, adsorption kinetic, composite adsorbent, nickel, zinc

Haider M. Zwain
College of Water Resources Engineering,
Al-Qasim Green University,
Al-Qasim Province, Babylon,
Iraq

Mohammadtaghi Vakili
State Key Joint Laboratory of Environment Simulation and Pollution Control, Beijing Key Laboratory for Emerging Organic Contaminants Control, School of Environment,
Tsinghua University,
Beijing 100084,
China

Irvan Dahlan (corresponding author)
School of Chemical Engineering,
Universiti Sains Malaysia,
Engineering Campus, Seri Ampangan, Nibong Tebal, 14300 Nibong Tebal,
Malaysia
and
Solid Waste Management Cluster, Science and Engineering Research Centre,
Universiti Sains Malaysia,
Engineering Campus, Seri Ampangan, Nibong Tebal, 14300 Nibong Tebal,
Malaysia
E-mail: *chirvan@usm.my*

INTRODUCTION

The increased concentrations of heavy metals in the environment are a global problem. The World Health Organization (WHO) is concerned about drinking water that contains heavy metals like aluminum, manganese, chromium, cobalt, iron, nickel, zinc, copper, mercury, lead, and cadmium (WHO 2011). A part of that, Zn^{2+} and Ni^{2+} are among the most highly toxic heavy metals. Even at extremely low concentration, Ni^{2+} presents an environmental threat and causes cancer of lungs and nasal sinus (Ahmedna *et al.* 2004). On the other hand, Zn^{2+} is important for humans in small quantities, but it can affect health when the prescribed limit is exceeded. The World Health Organization (WHO 2011) has limited the concentrations of Zn^{2+} and Ni^{2+} to 3 mg/L and 0.07 mg/L, respectively. Most Zn^{2+} and Ni^{2+} enters the environment from various industrial effluents including cadmium–nickel batteries, lead and cadmium ores, purifying zinc, coal burning and burning of wastes, steel production, phosphate fertilizers, mining, alloy, pigments, and stabilizers (Low & Lee 1991).

There are many techniques available for heavy metals' removal such as adsorption reverse osmosis, solvent extraction, ion exchange and precipitation. Among these, adsorption using activated carbon is a well-known technique for heavy metals' removal, but the high cost of this technique limits its large-scale application in developing countries. In addition, many other adsorbents have been

doi: 10.2166/aqua.2018.150

developed from different industrial by-products for heavy metal removal. However, there is still the need to investigate the capability of low cost and efficient adsorbents, especially for the adsorption of Zn^{2+} and Ni^{2+} from aqueous solutions (Zwain *et al.* 2014).

Apart from producing heavy metal-containing wastewater, industrial activities also leave behind a great deal of solid waste in ash form. Some naturally occurring agriculture by-products may serve as low cost adsorbents for heavy metal removal because they are widely available in large quantities, represent unused resources, and are environmentally friendly. However, the adsorption capacity of adsorbents made of agricultural by-products is usually less than synthetic adsorbents, but these materials may offer cost-effective alternative technique for heavy metals' removal from water and wastewater (Zwain 2012; Kim & Lee 2015).

Many attempts have been made to utilize waste materials as an alternative adsorbent, especially waste-derived siliceous materials such as rice husk ash (RHA), palm oil fuel ash (PFA), and coal fly ash (CFA). Although RHA, PFA, and CFA have been investigated as adsorbents for pollutants' removal, most of the studies only use one type of ash (with or without modification) and other studies have converted these ashes into activated carbon before use as an adsorbent. Furthermore, no work has been conducted to synthesize a composite adsorbent out of these waste-derived siliceous materials.

In addition, an effective method was required to synthesize the composite RHA/PFA/CFA adsorbent. A previous study by Adam & Chua (2004) has shown that RHA adsorbents could be synthesized using sol-gel method in the presence of aluminum ion. They found that this silica-incorporated aluminum is a very promising adsorbent for palmitic acid adsorption. Metal oxides contained in RHA might be essential in the adsorption of this palmitic acid. Therefore, the objective of this research is to investigate the removal of Zn^{2+} and Ni^{2+} from aqueous solutions using composite RHA/PFA/CFA adsorbent prepared by sol-gel method. Several operating parameters, including adsorbent dosage, contact time, and pH were studied during batch adsorption experiment. The study also investigates the adsorption isotherms and adsorption kinetics.

EXPERIMENTAL

Adsorbent preparation

Three types of ash (i.e., RHA, PFA, and CFA) were collected from burning industrial fuels and used in the adsorbent preparation. RHA was obtained from Kilang Beras & Minyak Sin Guan Hup Sdn. Bhd., Pulau Pinang, Malaysia. PFA was supplied directly by United Oil Palm Mill, Pulau Pinang, Malaysia. CFA was collected from Stesen Janakuasa Sultan Azlan Shah, Manjung, Perak, Malaysia. Prior to use, the ashes were sieved to a fine particle size of less than 63 μm and then dried in an oven overnight at 110 °C.

Adsorbent was prepared by sol-gel method (Adam *et al.* 2006). About 15 g of each ash (RHA, PFA, CFA) was mixed and stirred in nitric acid (HNO_3 65%) for 24 h. The mixture was filtered, rinsed with distilled water until the pH of the rinse became constant, and then dried in an oven at 110 °C for 1 day. About 15 g of the acidified RHA/PFA/CFA adsorbent was dissolved in 250 mL of 6 M NaOH, stirred for 12 h, and then filtered to eliminate insoluble particles. Thereafter, the filtrant was titrated with 3 M HNO_3 that contained 10% (w/w) aluminum ion [Al $(NO_3)_3.9H_2O$ in HNO_3]. When the pH reached 11.5, a black suspension was seen, then titration was carried out until the pH reached 5. Finally, the RHA/PFA/CFA composite adsorbent was kept for 6 days, then the forming soft gel was filtered and oven dried at 110 °C for 1 day.

In this study, the synthetic wastewater was prepared by dissolving 132 mg of $ZnSO_4.7H_2O$ and 124 mg of $Ni(NO_3)_2.6H_2O$ in 1 L of deionized water to achieve Zn^{2+} and Ni^{2+} concentrations of 30 ± 2 mg/L and 25 ± 2 mg/L, respectively. This synthetic wastewater represents Zn^{2+} and Ni^{2+} concentrations in metal plating industries wastewater (Bayat 2002). The elements of RHA, PFA, and CFA were analyzed by X-ray photoelectron spectrometer (XPS, PHI 1600). The properties of the composite RHA/PFA/CFA adsorbent were also investigated using Fourier transform infrared (FTIR), specific surface area and particle size distribution. The surface functional groups of the adsorbent were detected using FTIR spectroscopy (Perkin Elmer, spectrum 100 Series model). The spectra were recorded from 4,000 to 400 cm^{-1}. Particle size distribution and

specific surface area of the composite RHA/PFA/CFA adsorbents were examined using Mastersizer 2000.

Adsorption studies

The experiments of adsorption process were carried out at ambient temperature (27 ± 2 °C) in a batch mode. The contents of five 250 mL flasks holding 100 mL of Zn^{2+} and Ni^{2+} synthetic wastewater were first mixed with 2, 4, 6, 8, and 10 g/L of the RHA/PFA/CFA adsorbents. The samples were stirred in SK-600 horizontal shaker at 110 rpm, neutral pH of 6, and contact time of 60 min. After an optimum adsorbent dosage of 10 g/L had been selected, the batch experiment was then continued by changing the contact time from 10 to 60 min, stirred at 110 rpm and neutral pH of 6. Using the optimum conditions from the previous experiments (adsorbent amount of 10 g/L and contact time of 60 min), pH of the solution was then changed from 3 to 9. At each experiment, the equilibrium condition was predicted by drawing samples at certain periods of time until there was a minor change in removal efficiency. Throughout the experiment, 5 mL of the synthetic wastewater was taken at certain time periods, and the concentrations of Zn^{2+} and Ni^{2+} were tested using a DR 2500 Spectrophotometer. The amount of Zn^{2+} and Ni^{2+} adsorbed (mg/L) was recorded based on the change in the concentrations of Zn^{2+} and Ni^{2+} before and after the adsorption process, and shown by Equation (1) below:

$$\text{RE}\,\% = \frac{C_o - C_e}{C_o} \times 100 \tag{1}$$

where C_o is the initial metal concentration (mg/L) and C_e is the final metal concentration (mg/L) at equilibrium. All the batch experiments were tested three times to increase the data precision, and only the average values of Zn^{2+} and Ni^{2+} concentrations were reported throughout this study.

Adsorption isotherm studies

Isotherm studies were conducted using five flasks (250 mL), in which synthetic wastewater (100 mL) contained 30 ± 2 mg/L of Zn^{2+} and 25 ± 2 mg/L of Ni^{2+}. The solution pH was kept constant at 6.5. Different amounts of RHA/PFA/CFA adsorbent (0.2–1 g) were mixed with the synthetic wastewater, and were placed in SK-600 horizontal shaker for 60 min until it reached equilibrium. After certain periods, the samples were filtered and the concentrations of heavy metals were analyzed using DR 2500 spectrophotometer. The adsorption capacity (q_e mg/g) at equilibrium time (t), is calculated by

$$q_e = \frac{(C_o - C_e) \times V}{W} \tag{2}$$

where C_o is the initial metal concentration (mg/L), C_e is the final metal concentration (mg/L) at equilibrium, V is the sample volume (L), and W is the weight of RHA/PFA/CFA adsorbent (g).

Adsorption kinetic studies

Kinetic studies were conducted in a series of flasks (250 mL). The metal ion solutions were withdrawn at prescribed time intervals, i.e., 10–60 min, filtered and analyzed for heavy metal concentrations using DR 2500 spectrophotometer. The adsorption capacity q_t (mg/g) at time (t), is determined by the following equation:

$$q_t = \frac{(C_o - C_t) \times V}{W} \tag{3}$$

where C_o is the initial metal concentration (mg/L), C_t is the metal concentration (mg/L) at any time (t), V is the sample volume (L), and W is the weight of RHA/PFA/CFA adsorbent (g).

RESULTS AND DISCUSSION

Adsorbent characterization

In this study, a composite RHA/PFA/CFA adsorbent was made by combining three different types of ash together. RHA contains 63% of SiO_2, 19% of C, and other metallic elements in minor quantities; PFA contains about 34% of SiO_2, 25% of C, 6% of Al_2O_3, 5% of CaO, and other amounts of metallic elements; and CFA contains about 31% of SiO_2,

24% of C, 11% of Al_2O_3, 10% of Fe_2O_3, 7% of CaO, and other metallic components. The characteristics of composite RHA/PFA/CFA adsorbent have been investigated using FTIR, particle size distribution and specific surface area. Figure 1 shows the corresponding FTIR spectrums of the composite RHA/PFA/CFA adsorbent. The FTIR absorption bands appearing at 465, 797, and 1,053 cm^{-1} are assigned with Si–O groups, attributed to bending of Si–O, symmetric stretching vibration of the Si–O (quartz), and asymmetric stretching vibration of the Si–O, respectively (Muller *et al.* 2014). According to the preparation process, the peak at around 1,384 cm^{-1} is attributed to the NO_3- group, while the peak at 1,635 cm^{-1} is assigned to H–OH bending of water molecules trapped in the silica matrix. The absorption peak around 3,436 cm^{-1} is associated with the O–H stretching vibration from the solid Si–OH and the HO–H vibration of the water molecules adsorbed on the silica surface (Adam & Chua 2004).

The composite RHA/PFA/CFA adsorbent was also analyzed for particle size distribution and surface area, and the results are presented in Figure 2. The composite RHA/PFA/CFA adsorbent had a bimodal particle size distribution, with a predominance of particles in the range of 1–91 μm (averaged at 25 μm), followed by particles in the range 240–630 μm (averaged at 450 μm). This might be due to the combination of different materials (i.e., RHA, PFA, and CFA), influenced by the preparation process using the sol-gel method, leading to large particles' breakup or variable growth mechanisms during the preparation method. Adsorbents with bimodal particle size distribution

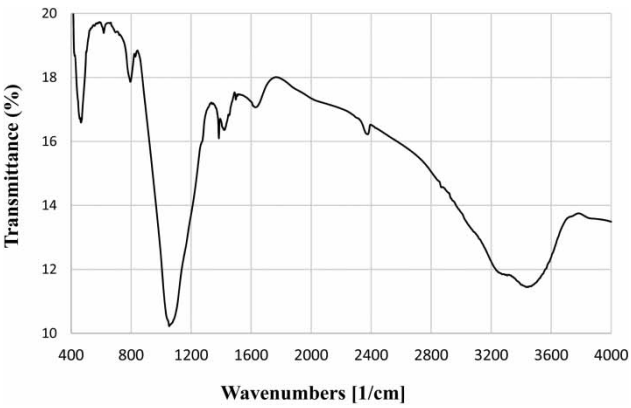

Figure 1 | The FTIR spectrum of composite RHA/PFA/CFA adsorbent.

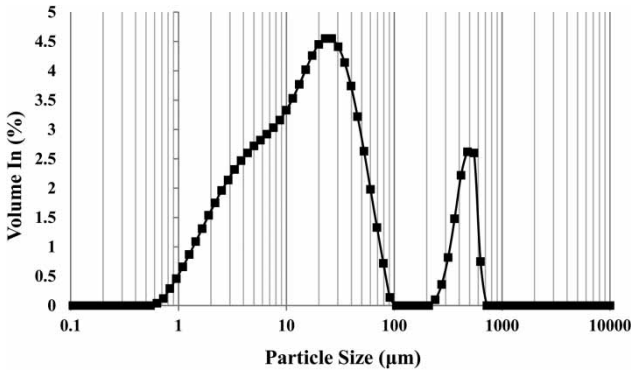

Figure 2 | Particle size distribution of composite RHA/PFA/CFA adsorbent.

have a higher adsorption capacity than unimodal particle size distribution. Sim *et al.* (2014) reported that an adsorbent with bimodal structure showed a higher uptake capacity and faster adsorption rate of silver ion and silver nanoparticles. The bimodal particle size distribution of the composite RHA/PFA/CFA adsorbent structure enables enhanced capillary driven aqueous solution distribution without hindering the aqueous solution intake of the adsorbent core.

In addition, the composite RHA/PFA/CFA adsorbent had a specific surface area of 77.4 m^2/g. In comparison, the specific surface areas of RHA, PFA, and CFA prior to treatment were 11.35 m^2/g (Fernandes *et al.* 2017), 1.775 m^2/g (Megat Johari *et al.* 2012), and 1.1 m^2/g (Xie *et al.* 2014), respectively. There is a notable difference in specific surface area between individual ashes and the composite RHA/PFA/CFA adsorbent, which might be due to the preparation using the sol-gel method and the combination of different materials. Specific surface area is defined as the sum of total area of particles including pores, and has been directly correlated with particle size and porosity. Smaller, highly porous particles have considerable surface area, while larger, non-porous ones have reduced surface area values (Fernandes *et al.* 2017).

Effect of adsorbent amount

By varying the adsorbent amounts from 2 to 10 g/L, the effect of the adsorbent amount was investigated. Table 1 provides the experimental data for Zn^{2+} and Ni^{2+} adsorption. For all experiments, the concentration of initial

Table 1 | The experiment data of adsorption process at different batches

	Zn^{2+}			Ni^{2+}		
	C_o (mg/L)	C_e (mg/L)	Removal efficiency (%)	C_o (mg/L)	C_e (mg/L)	Removal efficiency (%)
Adsorbent amount[a] (g/L)						
2	30	18.8	41	25	18.6	26
4	30	13.0	59	25	14.6	42
6	30	9.3	71	25	12	52
8	30	7.2	78	25	10	60
10	30	6.0	81	25	8.6	66
12	30	7.0	78	25	9	64
Contact time[b] (min)						
10	30	14.2	56	25	19	24
20	30	8.7	73	25	15.4	38
30	30	7.3	77	25	13.2	47
40	30	7	78	25	12	52
50	30	6.4	80	25	11.1	56
60	30	6.2	81	25	10.7	57
pH[c]						
3	30	12.8	60	25	19.2	23
5	30	7.25	77	25	14.7	41
7	30	1.3	96	25	10.2	59
9	30	0.65	98	25	4.2	83

[a]Initial Zn^{2+} and Ni^{2+} concentration of 30 ± 2 mg/L and 25 ± 2 mg/L, respectively, shaker rate of 110 rpm, neutral pH of 6 and contact time of 60 min.
[b]Initial Zn^{2+} and Ni^{2+} concentration of 30 ± 2 mg/L and 25 ± 2 mg/L, respectively, shaking rate of 110 rpm, neutral pH of 6 and adsorbent dosage of 10 g/L.
[c]Initial Zn^{2+} and Ni^{2+} concentration of 30 ± 2 mg/L and 25 ± 2 mg/L, respectively, shaking rate of 110 rpm, contact time of 60 min and adsorbent dosage of 10 g/L.

metal ions was fixed at 30 ± 2 mg/L of Zn^{2+} and 25 ± 2 mg/L of Ni^{2+}. Figure 3 shows the adsorption of Zn^{2+} and Ni^{2+} ions increases rapidly with increasing the amount of RHA/PFA/CFA adsorbent. The major increase in Zn^{2+} and Ni^{2+} removal was noticed from 41 to 81% and 25 to 66% when the adsorbent amount was increased from 2 to 10 g/L, respectively. Increasing the adsorbent amount will increase the availability of surface area and binding sites on the adsorbent surface. In addition, RHA, PFA, and CFA contain carbon and silica based substances that attach the metal ion to each other in an aqueous solution (Dahlan *et al.* 2007, 2008; Lee *et al.* 2008).

The results showed that the removal efficiency for Zn^{2+} ions is higher than for Ni^{2+} ions. This might indicate that the

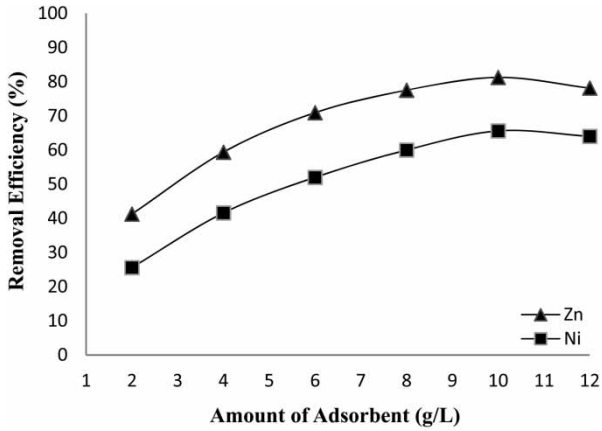

Figure 3 | Effect of adsorbent amount on Zn^{2+} and Ni^{2+} adsorption by composite adsorbent. Initial Zn^{2+} concentration of 30 ± 2 mg/L, initial Ni^{2+} concentration of 25 ± 2 mg/L, shaker rate of 110 rpm, neutral pH of 6, and contact time of 60 min.

surface of composite RHA/PFA/CFA adsorbent has a higher affinity for Zn^{2+} ions than for Ni^{2+} ions. This could be associated with the adsorbent pore size, which is more favorable for smaller atomic size of Zn^{2+} ions (139 pm) than Ni^{2+} ions (163 pm) (Enghag 2008). In addition, higher charge density on the surface of smaller sized Zn^{2+} ions could also be another reason for their higher removal efficiency compared to Ni^{2+} ions.

The results also showed that maximum removals of Zn^{2+} and Ni^{2+} were obtained at adsorbent amount of 10 g/L. After that, the adsorbent uptake efficiency reached equilibrium condition without further increase. Therefore, the next adsorption studies were conducted using adsorbent amount of 10 g/L. At high adsorbent amount, the available heavy metal concentration is insufficient to cover the exchangeable available sites on the adsorbent, resulting in low metal adsorption. Further, increased adsorbent amount leads to an interference between binding sites and may result in a low specific removal. The interactions between heavy metal ions become more essential when the adsorbent amount in the liquid phase is higher, as this may cause physical blockage of some adsorption sites, leading to a decreased adsorption efficiency. These interactions can result in electrostatic interferences, where the electrical surface charges on the closely packed particles diminish attractions between the surfaces of individual grains and adsorbed solutes (Malamis & Katsou 2013).

Effect of contact time

Table 1 shows the adsorption of Zn^{2+} and of Ni^{2+} onto RHA/PFA/CFA adsorbent while varying the contact time. Adsorption of Zn^{2+} and of Ni^{2+} is highly enhanced by increasing the contact times from 10 to 60 min. Figure 4 shows that the adsorption of Zn^{2+} and Ni^{2+} rapidly increased in the first 30 min, where about 77% of Zn^{2+} and 41% of Ni^{2+} was removed, after which, equilibrium was slowly reached. This could be due to the excessively adsorbent surface area available at the start of the Zn^{2+} and Ni^{2+} adsorption process (Bhattacharya *et al.* 2006). Similarly, Rashid *et al.* (2016) reported that the removal of Zn^{2+} and Ni^{2+} was faster in the beginning and slowed down until equilibrium was reached. They reported that the adsorption process occurred in two stages: initial shorter duration (fast stage), followed by longer second duration (slower stage); then it continued until equilibrium was achieved.

When the adsorbent surface area becomes limited, further increase in adsorption capacity is associated with the transport of adsorbate from the exterior to the interior sites of the adsorbent substances (Dahlan & Zwain 2013). Increment in contact time has increased the Zn^{2+} and Ni^{2+} adsorption, but it remains unchanged after reaching equilibrium in 40 min and 50 min for Zn^{2+} and Ni^{2+}, respectively. Moreover, the maximum Zn^{2+} and Ni^{2+} removal efficiencies of 81% and 60%, respectively, were attained at contact time of 60 min. Likewise, Kara *et al.* (2017) mentioned that Zn^{2+} and Ni^{2+} adsorption reached equilibrium at 40 and 50 min, with adsorption capacity of 60.06 mg/g and 29.40 mg/g, respectively.

Effect of pH

The pH of solution highly affects the adsorption process due to the speciation of adsorbate species, degree of ionization, and changes of charge on adsorbent surface. Figure 5 shows the effect of pH level (range 3–9) on adsorption of Zn^{2+} and Ni^{2+} by RHA/PFA/CFA adsorbent. It was found that the adsorption process was strongly dependent on the pH level presented in the media. When the pH increased from 3 to 7, there was a sharp increase in adsorption process from 60% to 96% and from 23% to 59% for Zn^{2+} and Ni^{2+}, respectively. In pH from 7 to 9, no change was observed in the removal of zinc due to the fact that most of the Zn^{2+} ions were removed earlier. In contrast, the Ni^{2+} adsorption further increased from 59% to 83% when pH level increased from 7 to 9, however, the Zn^{2+} adsorption was higher than Ni^{2+}. Thus, pH 7 was taken into account as the optimum pH level for the following studies.

At different pH values, the difference in adsorption of Zn^{2+} and Ni^{2+} by RHA/PFA/CFA adsorbent could be due to different surface charges resulting from different adsorbent surface and different degrees of solute speciation ionization (Rashid *et al.* 2016). At extremely acidic and

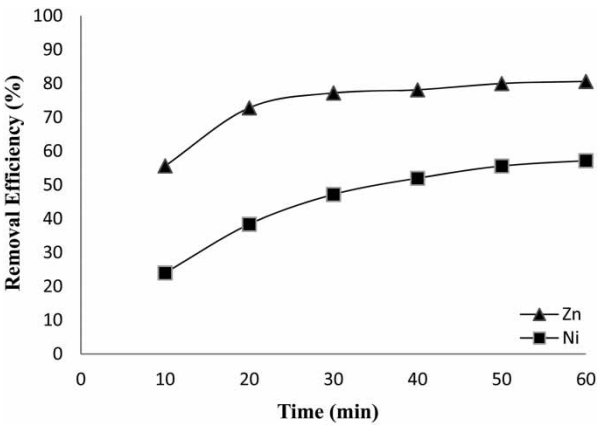

Figure 4 | Effect of contact time on Zn^{2+} and Ni^{2+} adsorption by composite adsorbent. Initial Zn^{2+} concentration of 30 ± 2 mg/L, initial Ni^{2+} concentration of 25 ± 2 mg/L, shaking rate of 110 rpm, neutral pH of 6, and adsorbent dosage of 10 g/L.

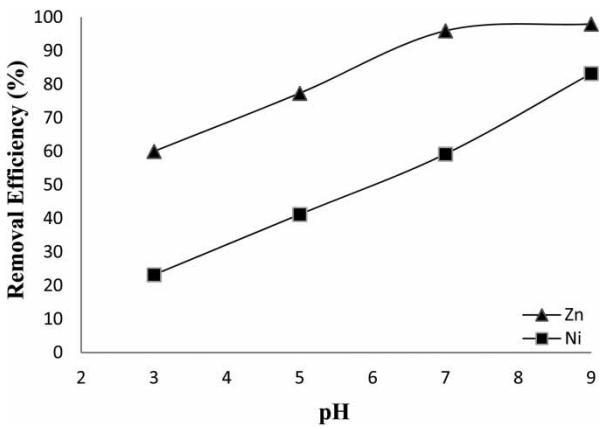

Figure 5 | Effect of pH on Zn^{2+} and Ni^{2+} adsorption by composite adsorbent. Initial Zn^{2+} concentration of 30 ± 2 mg/L, initial Ni^{2+} concentration of 25 ± 2 mg/L, shaking rate of 110 rpm, contact time of 60 min, and adsorbent dosage of 10 g/L.

basic pH, low adsorption of metal ions could be due to sorbate lyophobic behavior. The functional groups are a key factor for metal binding, which could be affected by pH through protonation/deprotonation, leading to a decrease/increase in the attraction of charged metal ions (Ullah *et al.* 2013). In addition, at low level of pH, there is practically less removal of metal ions due to the high electrostatic repulsion caused by high H^+ ion concentration on the surface sites. When the pH is increasing, the H^+ ion concentration on the adsorption site is reduced, resulting in decreased electrostatic repulsion, thus leading to an improvement of metal ions adsorption (Aklil *et al.* 2004). On the other hand, at higher levels of pH, OH^- competes for Zn^{2+} and Ni^{2+} with the active sites on the surface of adsorbent and formation of the precipitate of $Zn(OH)_2$ and $Ni(OH)_2$ occurs and contributes to the removal process (Kalyani *et al.* 2003). To prevent metal ion precipitation, the rest of the following experiments were conducted at levels of pH not higher than 7.

Adsorption isotherm

Adsorption isotherm is a key factor to understand the distribution of adsorbate molecules between the solid phase and the liquid phase when the adsorption progress approaches the equilibrium condition. In addition, appropriate correlation of equilibrium curves is an important element to optimize the adsorption system design (Hasan *et al.* 2008). Many isotherm equations have been proposed for the sake of explaining the equilibrium conditions of adsorption. To elucidate the heterogeneous and homogeneous adsorption, Langmuir and Freundlich adsorption isotherms are proposed, respectively (Vakili *et al.* 2015). The linear equation of the Langmuir isotherm (Langmuir 1918) is described as:

$$\frac{C_e}{q_e} = \frac{1}{Q_o b} + \frac{C_e}{Q_o} \tag{4}$$

where q_e is the heavy metal amount in the adsorbent (mg/g) and C_e is the heavy metal concentration in the solution (mg/L) at equilibrium. The constant Q_o is the adsorption capacity (mg/g) and b signifies the energy of the adsorption (L/mg). Figure 6 shows the plotted straight line of C_e/q_e versus C_e whereby the intercept $1/Q_o$ b and slope $1/Q_o$

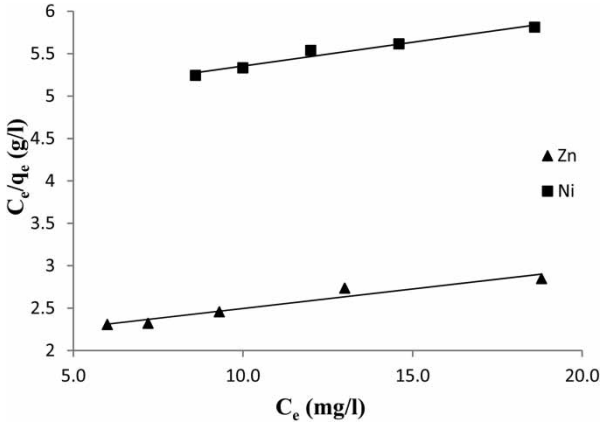

Figure 6 | Linear presentation plot of Langmuir isotherm for Zn^{2+} and Ni^{2+} adsorption by composite adsorbents. Initial Zn^{2+} concentration of 30 ± 2 mg/L, initial Ni^{2+} concentration of 25 ± 2 mg/L, shaking rate of 110 rpm, contact time of 60 min, and adsorbent dosage of (2–10 g/L).

can be obtained. Table 2 lists the calculated maximum adsorption capacity Q_o of heavy metal onto the RHA/PFA/CFA adsorbent.

Langmuir isotherm model is used to theoretically estimate the maximum metal removal that cannot be obtained in experimental studies. From this Langmuir isotherm model study, the maximum adsorption capacities (Q_o) were 21.74 and 17.85 mg/g for Zn^{2+} and Ni^{2+}, respectively. As compared to the actual adsorption capacities of 6.6 mg Zn^{2+}/g and 3.2 mg Ni^{2+}/g (measured at adsorbent amount of 2 g/L, contact time of 60 min, shaker rate of 110 rpm, neutral pH of 6, and initial Zn^{2+} and Ni^{2+} concentration

Table 2 | Summary for isotherm model constants and coefficient of determination for Zn^{2+} and Ni^{2+} adsorption onto composite adsorbent

Langmuir isotherm	b (L/mg)	Q_o (mg/g)	R_L	Equation	R^2
Zn^{2+}	0.022	21.74	0.58	$y = 0.046C + 2.035$	0.936
Ni^{2+}	0.011	17.85	0.78	$y = 0.056C + 4.793$	0.964
Freundlich isotherm	K_F	1/n		Equation	R^2
Zn^{2+}	0.64	0.79		$y = 0.794C - 0.454$	0.997
Ni^{2+}	0.25	0.87		$y = 0.866C - 1.370$	0.999
Temkin isotherm	K_T (L/mg)	B_1		Equation	R^2
Zn^{2+}	0.34	3.4		$y = 3.408C - 3.668$	0.977
Ni^{2+}	0.25	2		$y = 2.019C - 2.769$	0.988

of 30 ± 2 mg/L and 25 ± 2 mg/L, respectively), those values (Q_o) show that the RHA/PFA/CFA adsorbent did not reach its equilibrium condition. Hence, less amount of adsorbent could be used efficiently to remove these concentrations of metals (Vakili *et al.* 2016). The difference in adsorption capacities might be due to the different interaction mechanisms associated with different heavy metal ions. The affinity constant (b) for Zn^{2+} (0.022) was much higher than that for Ni^{2+} (0.011). Thus, the RHA/PFA/CFA adsorbent showed high affinity for the removal of Zn^{2+} (Table 2).

In addition, the fundamental feature of the Langmuir isotherm is signified as a dimensionless constant separation factor R_L shown by Webi & Chakravort (1974):

$$R_L = \frac{1}{1 + C_o b} \tag{5}$$

where C_o is the highest initial concentration of heavy metals (mg/L) and b is the Langmuir constant. The isotherm shape may be interpreted according to the value of R_L as follows: $R_L > 1.0$ is unfavorable, $R_L = 1.0$ is linear, $0 < R_L < 1.0$ is favorable, and $R_L = 0$ is irreversible. In this study, the dimensionless factor (R_L) was 0.58 and 0.78 for Zn^{2+} and Ni^{2+}, respectively. This result reveals favorable adsorption progress for both Zn^{2+} and Ni^{2+}.

The Freundlich isotherm is based on adsorption heterogeneous surfaces, where the exponential distribution of active sites and their energies and adsorption enthalpy changes logarithmically (Freundlich 1906). A linear form of the Freundlich equation is given by the following equation:

$$\ln q_e = \ln K_F + \frac{1}{n} \ln C_e \tag{6}$$

where q_e is the adsorbed amount (mg/g), C_e is the heavy metal concentration (mg/L) at equilibrium, K_F and n are Freundlich constants with K_F (mg/g $(1/mg)^{1/n}$) being the adsorbent capacity and n is a sign of favorability of adsorption process. The constant K_F and exponent n can be determined from Figure 7 ($\ln q_e$ versus $\ln C_e$).

K_F represents the distribution coefficient of Zn^{2+} and Ni^{2+} adsorbed by RHA/PFA/CFA adsorbent at equilibrium concentration. The slope $1/n$ is ranged between 0 and 1.0 which measures the surface heterogeneity or adsorption intensity. As the value of the slope approaches zero, the

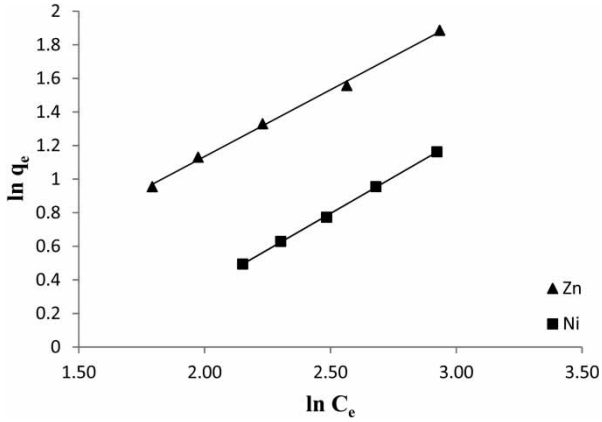

Figure 7 | Linear presentation plot of Freundlich isotherm for Zn^{2+} and Ni^{2+} adsorption by composite adsorbent. Initial Zn^{2+} concentration of 30 ± 2 mg/L, initial Ni^{2+} concentration of 25 ± 2 mg/L, shaking rate of 110 rpm, contact time of 60 min, and adsorbent dosage of (2–10 g/L).

adsorption surface become more heterogeneous. On the other hand, the adsorption surface become more homogenous when the slope gets closer to 1.0. The data of $1/n$ together with the coefficient of determination are presented in Table 2. In this study, the values of $1/n$ were 0.79 and 0.87 for Zn^{2+} and Ni^{2+}, respectively. This result indicates that the surface of RHA/PFA/CFA adsorbent is less heterogeneous. In general, the Freundlich equation is an empirical analysis for very uneven adsorbent surface that can adsorb single adsorbate at a fixed range of concentration.

In addition, Temkin & Pyzhev (1940) proposed an alternative equation to analyze isotherms using a factor that clearly considers adsorbing species to adsorbate interactions. This isotherm presumes the following: (i) the adsorption heat of all the molecules in the layer decreases linearly with coverage due to adsorbate–adsorbate interactions; and (ii) adsorption is characterized by a uniform distribution of binding energies, up to some maximum binding energy (Hasan *et al.* 2008). The linear form of Temkin isotherm is signified by the following equation:

$$q_e = B_1 \ln K_T + B_1 \ln C_e \tag{7}$$

The isotherm constants K_T and B_1 can be obtained from the q_e versus $\ln C_e$ plotting. K_T is the equilibrium binding constant (L/mg) related to the maximum binding energy and constant B_1 is correlated to the adsorption heat. Figure 8 shows the plotted Temkin isotherm with the parameter values listed in Table 2.

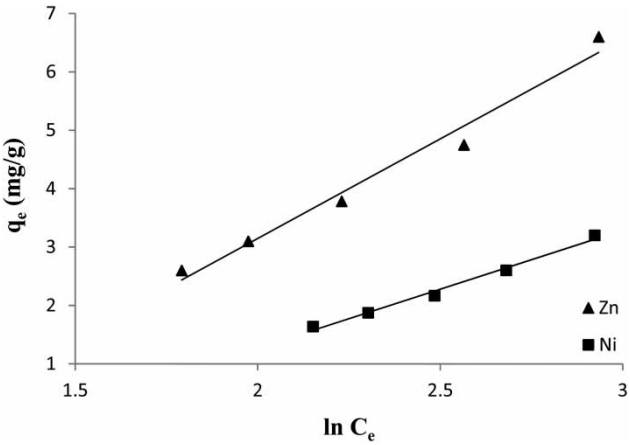

Figure 8 | Linear presentation plot of Temkin isotherm for Zn^{2+} and Ni^{2+} adsorption by composite adsorbent. Initial Zn^{2+} concentration of 30 ± 2 mg/L, initial Ni^{2+} concentration of 25 ± 2 mg/L, shaking rate of 110 rpm, contact time of 60 min, and adsorbent dosage of (2–10 g/L).

Considering the coefficient of determination (R^2) presented in Table 2, the adsorption isotherm study using the RHA/PFA/CFA adsorbent is explained by the Freundlich model followed by Temkin and Langmuir models. Additionally, the Freundlich model (Figure 7) better fits the experimental data than Temkin (Figure 8) and Langmuir models (Figure 6). The predicted equilibrium capacities of Zn^{2+} and Ni^{2+} onto RHA/PFA/CFA adsorbent using the Freundlich isotherm agrees precisely with the adsorption capacities of this experimental study. This suggests multilayer adsorption of Zn^{2+} and Ni^{2+} on less heterogeneous surfaces, and assumes that all of the active sites of the adsorbent participated in the adsorption processes.

Adsorption kinetics

In this study, pseudo-first-order and pseudo-second-order equations were used to explore the adsorption mechanism. The first rate equation was developed by Lagergren (1898) according to the solid capacity for adsorption in liquid/solid systems. The pseudo-first-order equation is presented by the following equation:

$$\log(q_e - q_t) = \log q_e - \frac{k_1}{2.303}t \tag{8}$$

where q_e and q_t are the heavy metal amounts adsorbed on adsorbent (mg/g) at equilibrium and at time t, respectively. The log (q_e – q_t) versus t was plotted and the slope and intercept determines the pseudo-first-order rate constant k_1 (1/min) (Figure 9).

The kinetic model for pseudo-second-order (Ho & McKay 1999) is presented as:

$$\frac{t}{q_t} = \frac{1}{k_2 q_e^2} + \frac{t}{q_e} \tag{9}$$

where k_2 (g/mg min) is the rate constant of pseudo-second-order. The applicability of pseudo-second-order kinetics is shown by linear relationship when plotting t/q_t versus t. From the plot of t/q_t versus t shown in Figure 10, the values of q_e and k_2 can be calculated from the slope and intercept, respectively, and it is not necessary to know any parameter beforehand.

The parameters (k_1, k_2) of this kinetic study are calculated and tabulated in Table 3. Based on the results presented in Figures 9 and 10, at initial concentrations of 30 ± 2 mg/L of Zn^{2+} and 25 ± 2 mg/L of Ni^{2+}, the adsorption kinetics of Ni^{2+} seems to obey both kinetic models, while adsorption kinetics of Zn^{2+} obeys only the pseudo-second-order kinetic model. In addition, from the coefficient of determination (R^2) values, pseudo-second-order model fits the data better than pseudo-first-order model for both Zn^{2+} and Ni^{2+} adsorption. Pseudo-second-order kinetic model assumes that chemisorption process may be the rate-limiting step. In chemisorption, the metal ions bind to the adsorbent surface, where a chemical (usually covalent)

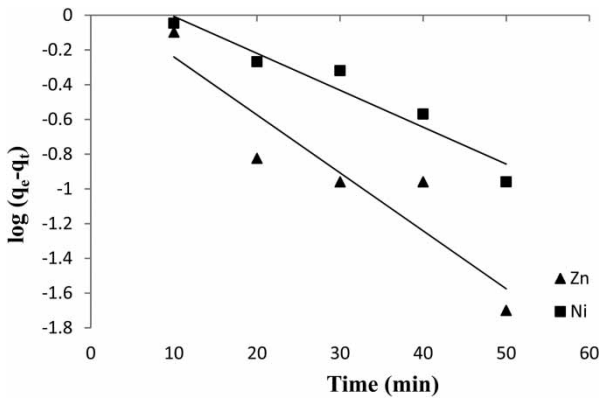

Figure 9 | Pseudo-first-order kinetics graph for Zn^{2+} and Ni^{2+} adsorption composite adsorbent. Initial Zn^{2+} concentration of 30 ± 2 mg/L, initial Ni^{2+} concentration of 25 ± 2 mg/L, shaking rate of 110 rpm, contact time of (10–60 min), and adsorbent dosage of 10 g/L.

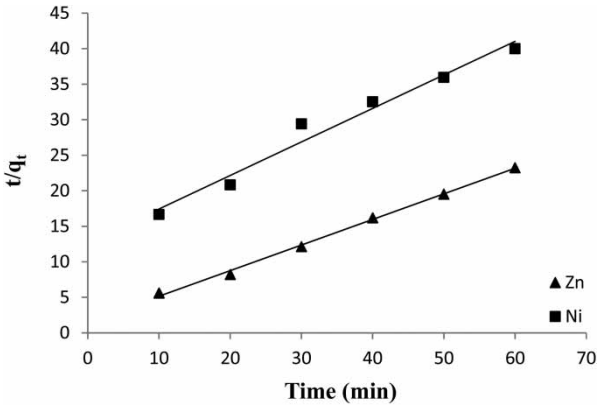

Figure 10 | Pseudo-second-order kinetics graph for Zn^{2+} and Ni^{2+} adsorption by composite adsorbent. Initial Zn^{2+} concentration of 30 ± 2 mg/L, initial Ni^{2+} concentration of 25 ± 2 mg/L, shaking rate of 110 rpm, contact time of (10–60 min), and adsorbent dosage of 10 g/L.

bond is formed, and look for sites that maximize their coordination number with the adsorbent surface (Atkins 1995).

Comparison of removal of Zn^{2+} and Ni^{2+} with different adsorbents

The adsorption capacities of RHA/PFA/CFA adsorbent removing Zn^{2+} and Ni^{2+} have been calculated, compared with different adsorbents given in the literature, and shown in Table 4. From Table 4, several studies using a single solid waste material (in the form of ash with/without modification) have been conducted to examine the adsorption of Zn^{2+} and Ni^{2+} using adsorbent prepared from rice husk ash (Bhattacharya *et al.* 2006), palm oil ash (Chu & Hashim 2003), and fly ash (Bayat 2002). In this work, the RHA/PFA/CFA adsorbent prepared by sol-gel method had a relatively high adsorption capacity (i.e., 21.74 mg/g and 17.85 mg/g for Zn^{2+} and Ni^{2+}, respectively), as compared

Table 3 | Kinetic parameters of cations adsorbed onto composite adsorbent at different adsorbent amounts

		Pseudo-first-order kinetic model			Pseudo-second-order kinetic model		
Cation	q_e exp. (mg/g)	q_e cal. (mg/g)	k_1 (1/min)	R^2	q_e cal. (mg/g)	k_2 (g/mg min)	R^2
Zn^{2+}	2.58	1.24	0.076	0.86	2.78	0.083	0.997
Ni^{2+}	1.5	1.67	0.048	0.932	2.12	0.017	0.973

Table 4 | Literature comparison in adsorption performance of Zn^{2+} and Ni^{2+} removal with different adsorbents

Metal	Adsorbent	q_{max} (mg/g)	References
Zn^{2+}	Rice husk ash	14.30	Bhattacharya *et al.* (2006)
Zn^{2+}	Palm oil ash	9.57	Chu & Hashim (2002)
Zn^{2+}	Fly ash	1.3	Bayat (2002)
Zn^{2+}	RHA/PFA/CFA (composite)	21.74	Present study
Ni^{2+}	Rice husk ash	14.6	Srivastava *et al.* (2007)
Ni^{2+}	Palm oil ash	9.9	Chu & Hashim (2003)
Ni^{2+}	Fly ash	1.16	Bayat (2002)
Ni^{2+}	RHA/PFA/CFA (composite)	17.85	Present study

to adsorbent prepared using a single solid waste material (with/without modification). The relatively high adsorption capacity shown by RHA/PFA/CFA adsorbent might be due to the interaction of silica between these solid waste materials to form more complex reactive species (Zwain & Dahlan 2012) that is responsible for Zn^{2+} and Ni^{2+} adsorption. On the other hand, among the three types of solid waste material which were prepared individually, rice husk ash had the highest Zn^{2+} and Ni^{2+} adsorption capacity. From this comparison, it shows that RHA/PFA/CFA adsorbent was more promising and efficient for Zn^{2+} and Ni^{2+} removal from aqueous solution.

CONCLUSIONS

This study confirmed that composite RHA/PFA/CFA adsorbent modified by the sol-gel method was an excellent adsorbent for removal of Zn^{2+} and Ni^{2+} from synthetic wastewater. The maximum adsorption capacity was observed at 10 g/L of adsorbent amount, 60 min of contact time, and pH 7 which gave 81% and 61% removal efficiency for Zn^{2+} and Ni^{2+}, respectively. An increase in adsorbent amount and contact time leads to an increase in adsorption efficiency. A decrease in pH level causes a major decrease in the adsorption capacity of Zn^{2+} and Ni^{2+}. The adsorption isotherm was found to best fit the Freundlich isotherm model for both Zn^{2+} and Ni^{2+}. The maximum adsorption capacity (q_{max}) calculated was 21.74 mg/g and 17.85 mg/g

for Zn^{2+} and Ni^{2+}, respectively. In addition, it was found that the pseudo-second-order model successfully explained the adsorption kinetics of Ni^{2+} and Zn^{2+}, as compared to the pseudo-first-order.

ACKNOWLEDGEMENTS

The authors are grateful for the Short Term Grant (A/C. 60310014) and Iconic Grant Scheme (A/C. 1001/CKT/870023) financial support received from Universiti Sains Malaysia.

REFERENCES

Adam, F. & Chua, J.-H. 2004 The adsorption of palmytic acid on rice husk ash chemically modified with Al(III) ion using the sol-gel technique. *Journal of Colloid and Interface Science* **280** (1), 55–61.

Adam, F., Kandasamy, K. & Balakrishnan, S. 2006 Iron incorporated heterogeneous catalyst from rice husk ash. *Journal of Colloid and Interface Science* **304** (1), 137–143.

Ahmedna, M., Marshall, W. E., Husseiny, A. A., Rao, R. M. & Goktepe, I. 2004 The use of nutshell carbons in drinking water filters for removal of trace metals. *Water Research* **38** (4), 1062–1068.

Aklil, A., Mouflih, M. & Sebti, S. 2004 Removal of heavy metal ions from water by using calcined phosphate as a new adsorbent. *Journal of Hazardous Materials* **112** (3), 183–190.

Atkins, P. W. 1995 *Physical Chemistry*, 5th edn. Oxford University Press, Oxford.

Bayat, B. 2002 Comparative study of adsorption properties of Turkish fly ashes: I. The case of nickel(II), copper(II) and zinc(II). *Journal of Hazardous Materials* **95** (3), 251–273.

Bhattacharya, A. K., Mandal, S. N. & Das, S. K. 2006 Adsorption of Zn(II) from aqueous solution by using different adsorbents. *Chemical Engineering Journal* **123** (1–2), 43–51.

Chu, K. H. & Hashim, M. A. 2002 Adsorption and desorption characteristics of zinc on ash particles derived from oil palm waste. *Journal of Chemical Technology and Biotechnology* **77** (6), 685–693.

Chu, K. & Hashim, M. 2003 Kinetic studies of copper (II) and nickel (II) adsorption by oil palm ash. *Journal of Industrial and Engineering Chemistry* **9** (2), 163–167.

Dahlan, I. & Zwain, H. M. 2013 A study on the removal characteristic of zinc ion (Zn^{2+}) from synthetic wastewater using a novel waste-derived siliceous sorbent. *Caspian Journal of Applied Sciences Research* **2** (AICCE'12 & GIZ' 12), 10–17.

Dahlan, I., Li, T. C., Lee, K. T., Kamaruddin, A. H. & Mohamed, A. R. 2007 Flue gas desulfurization using sorbent synthesized from lime (CaO) and oil palm ash (OPA) derived from empty fruit bunches (EFB): statistical design approach. *Environmental Engineering Science* **24** (6), 769–777.

Dahlan, I., Lee, K. T., Kamaruddin, A. H. & Mohamed, A. R. 2008 Analysis of SO_2 sorption capacity of rice husk ash (RHA)/CaO/NaOH sorbents using response surface methodology (RSM): untreated and pretreated RHA. *Environmental Science & Technology* **42** (5), 1499–1504.

Enghag, P. 2008 *Encyclopedia of the Elements: Technical Data-History-Processing-Applications*. John Wiley & Sons, Weinheim, Germany.

Fernandes, I. J., Sánchez, F. A. L., Jurado, J. R., Kieling, A. G., Rocha, T. L. A. C., Moraes, C. A. M. & Sousa, V. C. 2017 Physical, chemical and electric characterization of thermally treated rice husk ash and its potential application as ceramic raw material. *Advanced Powder Technology* **28** (4), 1228–1236.

Freundlich, H. M. F. 1906 Uber die adsorption in losungen. *Zeitschrift für Physikalische Chemie* **57**, 385–470.

Hasan, M., Ahmad, A. L. & Hameed, B. H. 2008 Adsorption of reactive dye onto cross-linked chitosan/oil palm ash composite beads. *Chemical Engineering Journal* **136** (2–3), 164–172.

Ho, Y. S. & McKay, G. 1999 Pseudo-second order model for sorption processes. *Process Biochemistry* **34** (5), 451–465.

Kalyani, S., Priya, J. A., Rao, P. S. & Krishnaiah, A. 2003 Adsorption of nickel on flyash in natural and acid treated forms. *Indian Journal of Environmental Health* **45** (3), 163–168.

Kara, İ., Yilmazer, D. & Akar, S. T. 2017 Metakaolin based geopolymer as an effective adsorbent for adsorption of zinc(II) and nickel(II) ions from aqueous solutions. *Applied Clay Science* **139**, 54–63.

Kim, H. K. & Lee, H. K. 2015 Coal bottom ash in field of civil engineering: a review of advanced applications and environmental considerations. *KSCE Journal of Civil Engineering* **19**, 1802–1818.

Lagergren, S. 1898 About the theory of so-called adsorption of soluble substances. *Kungliga Svenska Vetenskapsakademiens Handlingar* **24**, 1–39.

Langmuir, I. 1918 The adsorption of gases on plane surfaces of glass, mica and platinum. *Journal of the American Chemical Society* **40**, 1361–1403.

Lee, K. T., Tan, K. C., Dahlan, I. & Mohamed, A. R. 2008 Development of kinetic model for the reaction between SO_2/NO and coal fly ash/CaO/CaSO4 sorbent. *Fuel* **87**, 2223–2228.

Low, K. S. & Lee, C. K. 1991 Cadmium uptake by the Moss, Calymperes delessertii, Besch. *Bioresource Technology* **38** (1), 1–6.

Malamis, S. & Katsou, E. 2013 A review on zinc and nickel adsorption on natural and modified zeolite, bentonite and vermiculite: examination of process parameters, kinetics and isotherms. *Journal of Hazardous Materials* **252–253**, 428–461.

Megat Johari, M. A., Zeyad, A. M., Muhamad Bunnori, N. & Ariffin, K. S. 2012 Engineering and transport properties of high-strength green concrete containing high volume of ultrafine palm oil fuel ash. *Construction and Building Materials* **30** (Supplement C), 281–288.

Muller, C. M., Pejcic, B., Esteban, L., Delle Piane, C., Raven, M. & Mizaikoff, B. 2014 Infrared attenuated total reflectance spectroscopy: an innovative strategy for analyzing mineral components in energy relevant systems. *Scientific Reports* **4**, 6764.

Rashid, A., Bhatti, H. N., Iqbal, M. & Noreen, S. 2016 Fungal biomass composite with bentonite efficiency for nickel and zinc adsorption: a mechanistic study. *Ecological Engineering* **91**, 459–471.

Sim, J. H., Umh, H. N., Shin, H. H., Sung, H. K., Oh, S. Y., Lee, B.-C., Rengaraj, S. & Kim, Y. 2014 Comparison of adsorptive features between silver ion and silver nanoparticles on nanoporous materials. *Journal of Industrial and Engineering Chemistry* **20** (5), 2864–2869.

Srivastava, V. C., Mall, I. D. & Mishra, I. M. 2007 Adsorption thermodynamics and isosteric heat of adsorption of toxic metal ions onto bagasse fly ash (BFA) and rice husk ash (RHA). *Chemical Engineering Journal* **132** (1–3), 267–278.

Temkin, M. I. & Pyzhev, V. 1940 Kinetics of ammonia synthesis on promoted iron catalyst. *Acta Physicochimica, URSS* **12**, 327–356.

Ullah, I., Nadeem, R., Iqbal, M. & Manzoor, Q. 2013 Biosorption of chromium onto native and immobilized sugarcane bagasse waste biomass. *Ecological Engineering* **60**, 99–107.

Vakili, M., Rafatullah, M., Salamatinia, B., Ibrahim, M. H. & Abdullah, A. Z. 2015 Elimination of reactive blue 4 from aqueous solutions using 3-aminopropyl triethoxysilane modified chitosan beads. *Carbohydrate Polymers* **132**, 89–96.

Vakili, M., Rafatullah, M., Ibrahim, M. H., Abdullah, A. Z., Salamatinia, B. & Gholami, Z. 2016 Chitosan hydrogel beads impregnated with hexadecylamine for improved reactive blue 4 adsorption. *Carbohydrate Polymers* **137**, 139–146.

Webi, T. W. & Chakravort, R. K. 1974 Pore and solid diffusion models for fixed-bed adsorbers. *AIChE Journal* **20** (2), 228–238.

WHO 2011 *Guidelines for Drinking-Water Quality*, 4th edn. World Health Organization, Geneva, Switzerland.

Xie, J., Wang, Z., Wu, D. & Kong, H. 2014 Synthesis and properties of zeolite/hydrated iron oxide composite from coal fly ash as efficient adsorbent to simultaneously retain cationic and anionic pollutants from water. *Fuel* **116** (Supplement C), 71–76.

Zwain, H. M. 2012 *Comprehensive Study on Wastewater Treatment Using Low Cost Adsorbent*. Lambert Academic Publishing, Saarbrücken, Germany.

Zwain, H. M. & Dahlan, I. 2012 Characterization of RHA/PFA/CFA adsorbent and its equilibrium and kinetic studies for Zn^{2+} removal. *Caspian Journal of Applied Sciences Research* **1** (13), 23–34.

Zwain, H. M., Vakili, M. & Dahlan, I. 2014 Waste material adsorbents for zinc removal from wastewater: a comprehensive review. *International Journal of Chemical Engineering* **2014**, 13.

First received 21 September 2017; accepted in revised form 18 March 2018. Available online 5 April 2018